Published in final edited form as:
Biochim Biophys Acta. 2005 November 10; 1717(1): 41–49. doi:10.1016/j.bbamem.2005.09.006.

Effects of gramicidin-A on the adsorption of phospholipids to the air–water interface

Samares C. Biswas[a], **Shankar B. Rananavare**[b], and **Stephen B. Hall**[a,*]

[a]Departments of Molecular Biology and Biochemistry, Medicine, and Physiology and Pharmacology, Mail Code NRC-3, Oregon Health & Science University, Portland, OR 97239-3098, USA

[b]Department of Chemistry, Portland State University, Portland, OR 97207 and Department of Electrical and Computer Engineering, Oregon Graduate Institute of Science and Engineering, Beaverton, OR 97206, USA

Abstract

Prior studies suggest that the hydrophobic surfactant proteins, SP-B and SP-C, promote adsorption of the lipids in pulmonary surfactant to an air–water interface by stabilizing a negatively curved rate-limiting structure that is intermediate between bilayer vesicles and the surface film. This model predicts that other peptides capable of stabilizing negative curvature should also promote lipid adsorption. Previous reports have shown that under appropriate conditions, gramicidin-A (GrA) induces dioleoyl phosphatidylcholine (DOPC), but not dimyristoyl phosphatidylcholine (DMPC), to form the negatively curved hexagonal-II (H_{II}) phase. The studies reported here determined if GrA would produce the same effects on adsorption of DMPC and DOPC that the hydrophobic surfactant proteins have on the surfactant lipids. Small angle X-ray scattering and ^{31}P-nuclear magnetic resonance confirmed that at the particular conditions used to study adsorption, GrA induced DOPC to form the H_{II} phase, but DMPC remained lamellar. Measurements of surface tension showed that GrA in vesicles produced a general increase in the rate of adsorption for both phospholipids. When restricted to the interface, however, in preexisting films, GrA with DOPC, but not with DMPC, replicated the ability of the surfactant proteins to promote adsorption of vesicles containing only the lipids. The correlation between the structural and functional effects of GrA with the two phospholipids, and the similar effects on adsorption of GrA with DOPC and the hydrophobic surfactant proteins with the surfactant lipids fit with the model in which SP-B and SP-C facilitate adsorption by stabilizing a rate-limiting intermediate with negative curvature.

Keywords

Gramicidin; Lipid polymorphism; ^{31}P nuclear magnetic resonance; Pulmonary surfactant; Hydrophobic surfactant protein; Small angle x-ray scattering

1. Introduction

Pulmonary surfactant is the mix of lipids and proteins secreted by the type II pneumocytes that forms a thin film at the air–water interface of the alveolar air spaces. When compressed by the shrinking interfacial area during exhalation, the films reduce surface tension to remarkably low levels [1–5]. This function is essential for normal respiration. In premature

*Corresponding author. Tel.: +1 503 494 6667; fax: +1 503 494 7368. sbh@ohsu.edu (S.B. Hall).

babies who lack adequate amounts of surfactant, the increased surface tension collapses the alveoli, which then become injured during subsequent ventilation, leading to the flooded air spaces and respiratory failure of the Respiratory Distress Syndrome (RDS) [6].

Available evidence suggests that the surfactant films form rapidly. Immediately following birth when newborn babies first create the air–water interface, pulmonary mechanics are normal within the first few breaths [7]. In lungs made stiff by inactivation of surfactant during prolonged ventilation at a constant tidal volume, a single deep inspiration restores normal mechanics during the first exhalation [8]. Surfactant vesicles must therefore adsorb to create the interfacial film within seconds. The importance of the hydrophobic surfactant proteins, SP-B and SP-C, suggests that this rapid adsorption is essential. SP-B and SP-C greatly accelerate the adsorption of the surfactant lipids in vitro [9]. The congenital absence of SP-B, caused either by spontaneous defects [10] or genetic manipulation [11], produces RDS at birth despite normal amounts of the surfactant lipids. In mice that are genetically altered to allow control of SP-B expression after birth, the lungs become injured in adult animals when levels of the protein fall [12]. These results suggest that rapid adsorption of the surfactant vesicles, facilitated by the hydrophobic surfactant proteins, is required for normal respiratory function.

The studies reported here concern the possibility that the kinetics of adsorption are determined by the stability of a tightly-curved structure intermediate between the surfactant vesicles and the interfacial film. Unlike classical surfactants, which adsorb as individual molecules, the constituents of pulmonary surfactant insert collectively into the air–water interface as bilayer vesicles [13–15]. Constituents that promote adsorption, such as the hydrophobic surfactant proteins and the low-melting surfactant phospholipids, accelerate the process whether located exclusively in the vesicles or in preexisting films at the interface [16,17]. For the low-melting phospholipids, the beneficial effects in the two locations are identical [17]. These results strongly suggest that adsorption proceeds via an intermediate structure that is equally accessible from both locations. A structure analogous to the stalk-intermediate proposed for the fusion of two vesicles [18–20] represents one such possibility. The outer leaflet of the adsorbing vesicle would rupture to form two parts, each of which would fold back on itself to achieve the correct orientation for insertion of the phospholipids into the air–water interface [21]. These leaflets would then have the same inverse or negative curvature, concave on their polar face, that occurs in the hexagonal-II (H_{II}) phase. Consistent with this possibility, lipids that form the H_{II} phase adsorb rapidly [22,23]. The hydrophobic proteins might accelerate adsorption by inducing the same negative curvature.

The effects of compounds on the spontaneous curvature of lipid leaflets can be difficult to detect. Conflicting energetic considerations can frustrate the tendency of the lipids to bend [24], resulting in a bilayer in which the curvatures of the two opposing leaflets cancel to yield a planar structure. Consequently the spontaneous curvature of a leaflet, obtained in the absence of applied force, is inaccessible in systems such as pulmonary surfactant that form bilayers. Evidence that SP-B and SP-C tend to produce curvature is therefore limited [25].

The model, however, in which the hydrophobic surfactant proteins accelerate adsorption by stabilizing negatively curved structures, makes other predictions. Any peptide that induces the H_{II} phase should also facilitate adsorption. Gramicidin A (GrA) is a well-characterized, readily available membrane peptide that under appropriate conditions induces dioleoyl phosphatidylcholine (DOPC), but not dimyristoyl phosphatidylcholine (DMPC), to form the H_{II} phase [26–29]. The studies here first use small angle X-ray scattering (SAXS) and ^{31}P-nuclear magnetic resonance (NMR) to confirm that at a set of conditions appropriate for studying adsorption, mixtures of GrA with DOPC, but not with DMPC, form H_{II} structures. We then determine if under those conditions, GrA can replicate the changes in the

adsorption of those two lipids that the surfactant proteins produce in the adsorption of the surfactant lipids.

2. Materials and methods

2.1. Materials

Calf Lung Surfactant Extract (CLSE), prepared as described previously [30], was obtained from Dr. Edmund Egan (ONY, Inc., Amherst, NY). A preparation containing the complete set of Neutral and PhosphoLipids (N&PL) without the proteins was isolated from CLSE using gel permeation column chromatography [21,31]. GrA from Bacillus brevis of ≥90% purity was purchased commercially and used as received (Product Number 50845, Sigma-Aldrich Co, St. Louis, MO). DMPC and DOPC were obtained from Avanti Polar Lipids (Alabaster, AL), each found to produce a single spot on thin layer chromatography, and used without further purification. The concentration of phospholipid in stock solutions was determined by assay of total phosphate [32]. Water purified with a multicartridge system and exposure to dual wavelengths of ultraviolet light (Barnstead International, Dubuque, IA) contained low levels of organic contaminants (<2 ppb) and electrolyte (resistivity 18.2 MΩ-cm) and was used throughout the experimental work. All other chemicals and solvents used in these experiments were analytical grade.

2.2. Methods

2.2.1. Preparation of lipid vesicles—Samples of phospholipid and GrA were prepared at specific molar ratios by co-dissolving appropriate amounts of lipid and peptide in trifluoroethanol (TFE) and vortexing in round-bottom test tubes. After complete mixing, the solvent was evaporated with a stream of nitrogen. The resulting GrA/lipid film was placed in a vacuum desiccator overnight to remove the last trace of solvent, and then hydrated with 10 mM HEPES pH 7.0, 150 mM NaCl for an hour to a concentration of 30 mM phospholipid and resuspended by several cycles of sequential heating to 50 °C with vortexing for 3 min followed by cooling in an ice bath. The crude GrA/lipid vesicles were dispersed further in a water-bath sonicator for thirty min. The kinetics of adsorption were measured after overnight incubation of the sonicated vesicles. Samples of N&PL or CLSE for measurements of surface tension were prepared after drying appropriate amounts of material in chloroform. The completely dried film was then hydrated with 10 mM HEPES pH 7.0, 150 mM NaCl, 1.5 mM $CaCl_2$ and dispersed by the same methods used for GrA-lipid. Quasi-elastic light scattering (DynaPro Light-Scattering Instrument, Protein Solutions, Inc., Charlottesville, VA) was used to characterize the size of the dispersed particles.

2.2.2. Measurements of surface tension—Surface tension was measured using a force transducer (KSV Instruments Ltd., Helsinki, Finland) attached to a 0.3-cm-wide Wilhelmy paper plate. The microelectronic feedback system allowed the surface tension to be recorded directly to a computer using programs constructed with the graphical user interface LabVIEW (National Instruments, Austin, TX). The measurements used a Teflon beaker with a 4.0-cm^2 cross-section kept in a fully humidified chamber maintained at 37.0±0.5 °C with a circulating water bath. A fixed volume of 20 ml buffer was added to the Teflon beaker, and after temperature equilibration, 100 μl of vesicles at 30 mM phospholipid were injected into the subphase. After gently stirring for 15 min to provide complete mixing, adsorption to an initially clean interface was followed by measuring surface tension after removal of the interfacial film above the dispersed vesicles [21,33].

In experiments concerning the adsorption of lipid vesicles to preformed monolayers, lipid and peptide/lipid mixtures in solvent were spread at the air–water interface using a microsyringe (Hamilton, Reno, NV) to produce a final surface concentration of 1.02 μmol/

m^2 phospholipid. Experiments involving GrA used a spreading solvent of $CHCl_3$ for the phospholipids alone and 13:1 (v/v) $CHCl_3$/TFE for peptide/lipid mixtures. After incubation for 15–20 min to allow evaporation of spreading solvents, 100 μl of vesicles at 30 mM phospholipid without GrA were injected through a Teflon tube previously dipped into the subphase maintained at 37.0±0.5 °C. The subphase was stirred gently without disturbing the Wilhelmy plate to produce homogeneous mixing. Adsorption of N&PL vesicles to monolayers of N&PL or CLSE prespread from $CHCl_3$ with a surface concentration of 1.02 μmol/m^2 phospholipid was measured following injection of 100 μl N&PL dispersions at 20 mM phospholipid into the gently stirred subphase maintained at 37 °C.

Measurements of surface tension as a function of time are shown as representative curves to illustrate features that can be lost in averaged traces, with mean±S.D. for at least three experiments shown at selected points to indicate the variance of the data.

2.2.3. Small-angle X-ray scattering (SAXS)—A home-built X-ray diffractometer was used to measure SAXS from GrA-lipid mixtures. The instrument is equipped with an X-ray generator (XRD-3000, Phillips) operating at 45 kVand 20 mAwith a sealed fine-focus copper tube. The collimated monochromatic X-ray beam (λ =1.54 Å) was produced using a β-nickel filter and a pinhole collimator. The instrument was calibrated using lead stearate (d =49.8 Å) as the standard. Measurements were performed on GrA/ lipid vesicles at 30 mM phospholipid sealed in glass capillaries (1 mm diameter) maintained at 37.0±0.2 °C. The diffraction patterns were collected using a linear position-sensitive detector (spatial resolution of 92 μm/channel) interfaced to a personal computer through a multichannel analyzer (ND-53, Nuclear Data, Canbera Industries, Meriden, CT). Data were collected for each sample until the integrated intensity reached a common fixed value of 500,000 counts. The original data obtained as intensity versus channel number were converted to intensity versus q-spacing using the distances from sample to detector and from channel to the beam spot, along with the wavelength of the X-rays used for the measurement. To correct for small differences in intensity caused by the different capillary tubes, each set of data was normalized with respect to the peak immediately adjacent to the beam-block that results from scattering in air. Each diffraction peak was fit using a nonlinear least-squares routine to a Gaussian profile. Best-fit values yielded the peak position, intensity, and associated variances (3 S.D.).

2.2.4. Nuclear Magnetic Resonance (NMR)—Proton-decoupled ^{31}P-NMR spectra from non-spinning GrA-lipid dispersed samples at 30 mM phospholipid were collected on a spectrometer (AMX-400, Bruker, Billerica, MA) using ^{2}H-NMR as an internal lock. Each spectrum was collected at a probe temperature of 37 °C with 2000 scans at a 2-s repetition interval using a 15° pulse-width and 100 kHz sweep-width. A linewidth-broadening factor of 100 Hz was applied prior to Fourier transformation. Zero in the frequency domain corresponded to the chemical shift of phosphoric acid in D_2O. Chemical shift anisotropy (CSA) and lamellar volume fraction were determined by fitting simulated curves to the actual spectra using standard equations for an axially symmetric powder patterns and Lorentzian line-shapes for isotropic peaks [34]. Chemical shift anisotropies, line-widths and relative volume fractions were varied in a nonlinear least-squares program to obtain the optimal simulations. Inclusion of at most two kinds of line-shapes was sufficient to fit the spectra in all cases.

3. Results

3.1. Small angle X-ray scattering

Previous studies have shown that at the peptide/lipid ratios considered here, GrA can induce DOPC, but not DMPC, to form the H_{II} phase [26–29,35–37]. We first confirmed that the

same structural effects occurred for the particular conditions of temperature, composition and concentration that were convenient for studying adsorption. SAXS was measured for lipid alone and in combination with increasing amounts of GrA. Each phospholipid without peptide produced prominent first and second order peaks (Fig. 1), indicating the presence of a regularly repeating structure capable of diffraction. For the dispersed samples used in these measurements, the observed pattern of X-ray scattering suggested the formation of multilamellar vesicles. In the absence of GrA, the d-spacing, given by ($d=2\pi/q$), of the two peaks for both DMPC and DOPC occurred in a ratio close to the value of 2 (Table 1) expected for lamellar structures [38].

GrA produced different changes in the diffraction patterns for the two phospholipids (Fig. 1). For DMPC (Fig. 1A), the initial addition of GrA to 0.02 (mol/mol) GrA/lipid increased the intensity of the two peaks and their d-spacing, while maintaining the same d_1/d_2 ratio (Table 1). Additional GrA had no effect on the d-spacing, but the intensity of the peaks decreased. At 0.25 GrA/DMPC, the peaks were barely evident above noise. The d_1/d_2 ratio for all levels of GrA remained fixed at 2. With DOPC (Fig. 1B), GrA had little effect on the d-spacing of the first order peak, but the second peak broadened at 0.02 GrA/lipid, and then appeared in response to additional GrA at a different location. At and above 0.04 GrA/DOPC, d_1/d_2 closely approximated the value of $\sqrt{3}$ (Table 1) expected for the nonlamellar H_{II} phase [38]. GrA also produced a progressive decrease in the intensity of the diffraction peaks. SAXS, therefore, demonstrated that GrA decreased diffraction intensity with both phospholipids, but shifted the d_1/d_2 ratio from the lamellar to the H_{II} value [38] only with DOPC.

3.2. ^{31}P-NMR spectra from lipid vesicles

^{31}P-NMR spectroscopy provided a second method for determining microstructure in the lipid dispersions under the conditions used to study adsorption. Both pure lipids without GrA exhibited the axially symmetric powder pattern (Fig. 2), with a low-field shoulder and a high-field peak, that results from a lamellar structure [34]. Analogous to the results with SAXS, GrA produced different changes with the two lipids. With DMPC, GrA at 0.10 (mol/mol) peptide/lipid significantly reduced the chemical shift anisotropy (CSA) (Table 2), but preserved the same line-shape (Fig. 2A). The reduced CSA could reflect two processes. GrA could reorient the rotational axis of the phosphate group, or it could produce greater disorder [39,40]. A further increase in GrA to 0.25 peptide/ lipid produced a complex line-shape that suggested an isotropic peak, centered at 0 ppm, combined with the standard axially symmetric powder pattern of a lamellar phase. As with SAXS, ^{31}P-NMR showed no evidence of the H_{II} phase.

The addition of GrA to DOPC at a molar ratio of 0.10 changed the line-shape (Fig. 2B). Relative to DOPC alone, the symmetry of the spectrum was reversed, exhibiting the low-field peak and high-field shoulder that is characteristic of the H_{II} phase [34]. The altered line-shape, along with the SAXS results, confirmed that the hexagonal structure observed previously by other workers [27,35–37] was present under the conditions of our experiments. The width of the peak also decreased with GrA (Fig. 2B, Table 2) by 2.6, more than the factor of two expected for the simple shift from a lamellar to hexagonal phase [34]. Like the changes with DMPC at 0.10 GrA/lipid, the CSA could again reflect either reorientation of the phosphate group or greater disorder [39,40]. GrA therefore had additional structural effects beyond inducing DOPC to adopt the spontaneously curved hexagonal structures.

We also considered the possibility that the effect of GrA on CSA might reflect a decrease in vesicular size. Although the mechanism of the effect is debated [40], smaller particles of the same lipids have a reduced CSA. We used quasi-elastic light scattering to measure the

average hydrodynamic diameter for particles in the different GrA-lipid preparations. For samples containing GrA/DMPC ratios (mol/mol) of 0, 0.1 and 0.2, the diameter increased from 124 to 188 to 220 nm, respectively. With DOPC, the diameter decreased minimally from 246 nm for the pure lipid to 220 nm for 0.067 (mol/mol) GrA/DOPC, above which turbidity prevented accurate measurements. For all samples, the diameter remained well above the maximum value of 50 nm at which size should affect line-narrowing [39]. The decreased CSA with GrA, therefore, seemed unlikely to result from a change in size of the vesicles.

3.3. Adsorption: effect of hydrophobic proteins/peptides in vesicles

Our studies required that we determine if GrA can produce the same effects on the adsorption of phospholipids that the hydrophobic surfactant proteins have on the surfactant lipids. To document the role of the surfactant proteins, we compared the decrease in surface tension produced by the complete set of constituents extracted from calf surfactant (Calf Lung Surfactant Extract, CLSE) with adsorption of the Neutral and PhosphoLipids (N&PL), from which the proteins had been removed (Fig. 3). Gel permeation chromatography reduces the level of protein in N&PL to undetectable levels while maintaining the same set of phospholipid headgroups and acyl chains [31,41]. Dispersions made from N&PL adsorbed more slowly than CLSE. For N&PL, surface tension fell at continuously decreasing rates to 50 mN/m in 200 min. For CLSE dispersions, surface tension fell at rates that slowed until reaching 40–45 mN/m, but adsorption then accelerated until surface tension reached a final value of ~25 mN/m in 9 min. This late acceleration for CLSE produced an inflection point in the adsorption isotherm, which has been reported previously [21,42]. The hydrophobic surfactant proteins, therefore, produced not only a general acceleration of adsorption, but also a distinct late stage.

To determine if the effects of GrA on adsorption of DMPC and DOPC were comparable to those of the hydrophobic surfactant proteins on the surfactant lipids, we measured adsorption of phospholipid dispersions with a range of GrA/ lipid molar ratios (Fig. 4). The pure lipid dispersions, without GrA, adsorbed slowly. Incorporation of GrA in both cases produced a dose-dependent increase in the initial rate at which surface tension fell. The peptide with both DMPC and DOPC also generated the same late acceleration observed with CLSE (Fig. 4). At all GrA/lipid ratios, including for the pure lipids, the vesicles with DMPC (Fig. 4A) adsorbed more slowly than with DOPC (Fig. 4B). The qualitative effects of GrA with both phospholipids, however, were similar to each other and to the effects of the surfactant proteins on the surfactant lipids.

3.4. Adsorption: effects of proteins/peptides at the interface

Prior studies have shown that in addition to accelerating adsorption when present in vesicles of DPPC/DPPG, SP-B also promotes adsorption when confined to the air–water interface [16,43]. In experiments here with the complete set of surfactant lipids, the presence of the surfactant proteins exclusively in a preformed layer showed similar effects. N&PL vesicles adsorbed faster to a preexisting monolayer containing CLSE than to a film of N&PL without the proteins (Fig. 5).

To determine if GrA also promoted adsorption when restricted to the interface, we measured the adsorption of phospholipid vesicles, without GrA, to preformed monolayers containing a fixed surface concentration of the same lipid with different amounts of GrA (Fig. 6). For DMPC, the presence of GrA in the preformed film had no effect (Fig. 6A). With levels as high as 255 nmol/m^2, corresponding to a peptide/lipid ratio of 0.25, GrA produced no change in adsorption. GrA at the interface, however, did affect adsorption of vesicles containing only DOPC (Fig. 6B). With monolayers having the same phospholipid surface

concentration but also containing 102 nmol/m^2 or 255 nmol/m^2 GrA (GrA/DOPC ratios of 0.10 and 0.25, respectively), surface tension fell to the same final value obtained by GrA-DOPC vesicles within 40 and 10 min, respectively. Adsorption to the films with GrA also showed the late acceleration. When confined to the interface, GrA therefore replicated the qualitative effects of the surfactant proteins, but only with the lipid in which it formed the H_{II} phase, and not with DMPC that remained lamellar.

4. Discussion

Prior studies suggest that the hydrophobic surfactant proteins facilitate adsorption of the surfactant lipids by stabilizing a negatively curved structure that bridges the gap between the vesicles and the interface [21]. The outer lipid leaflet would fold back on itself to insert the lipids into the interface with the correct orientation. One hypothesis generated by the model is that other factors which stabilize negative curvature should produce the same functional consequence of faster adsorption. The current studies use induction of the H_{II} phase, not to demonstrate the presence of an essential equilibrium structure, but as an indication that with DOPC, GrA can stabilize the negative curvature that would be present in the proposed transient intermediate. Under conditions at which GrA induces DOPC to form the H_{II} phase, the peptide produces the same changes in adsorption that the hydrophobic proteins generate with the surfactant lipids. The correspondence of the structural and functional effects produced by GrA with DOPC therefore supports the model in which hydrophobic peptides such as the surfactant proteins stabilize the negatively curved intermediate.

The effects of the surfactant proteins at the interface provide crucial evidence for the model. In preexisting films, the surfactant proteins promote adsorption of vesicles that contain only lipids. Our results show that this observation, originally made with model lipids [16], extends to the complete set of surfactant lipids. The similar effects on adsorption of the proteins at the interface and in the vesicles strongly suggest that they affect a structure equally accessible from the two locations. The findings here, that a peptide can have the same effect under conditions at which it induces formation of the H_{II} phase, supports the importance of negative curvature in that bridging structure.

Both SAXS and ^{31}P-NMR indicate that with DOPC, GrA induces the H_{II} phase under the particular conditions of our adsorption experiments, and that the peptide therefore stabilizes a negatively curved structure. The mechanism by which the peptide produces that stabilization remains unspecified. One possibility is that GrA reduces the energy of bending. If a lipid leaflet can be considered as a continuum layer, then for weakly bent leaflets, the bending elastic energy per unit area, g, is given by:

$$g=\frac{1}{2}\kappa(c_1+c_2-c_o)^2+\bar{\kappa}c_1c_2$$

where c_o is the spontaneous curvature in the absence of applied force, c_1 and c_2 are the curvatures along the principal radii of the actual structure, and κ and $\bar{\kappa}$ are the curvature-elastic moduli of splay and saddle-splay, respectively [44–46]. Factors such as peptides could lower the bending energy by inducing a spontaneous curvature, by decreasing the elastic moduli, or by producing both effects.

Recent studies suggest that GrA affects c_o [47]. Determination of c_o requires evaluation of lipid structures containing individual unpaired leaflets, so that the tendency to bend is not frustrated in a bilayer by the opposing curvature of the other leaflet. GrA produces a dose-related decrease in the d-spacing of the H_{II} phase formed with DOPC, indicating that the peptide generates tighter curvature and a change in c_o [47].

Our NMR results suggest that in addition to affecting curvature of the DOPC leaflets, GrA also affects their flexibility by reducing κ. The CSA of ^{31}P-NMR depends on orientational averaging of the phospholipid headgroup, and is proportional to the orientational order parameter S [34,48]. Without other changes, reconfiguration of lipids from a planar to a cylindrical assembly reduces the CSA by a factor of two [34,49]. For our system, the change induced by GrA is somewhat larger. GrA therefore must produce an additional structural effect beyond the shift to the new phase. The greater-than-expected CSA could reflect a common reorientation of the phosphate groups within the leaflet, or an additional motional averaging of the phosphate head group. Although our experiments provide no definitive distinction between these two explanations, greater disorder would imply a more flexible leaflet. The orientational order parameter S is related to the bending modulus by $\kappa \alpha S^2$ [50,51], and therefore an increase in disorder would change κ. The ability of GrA to stabilize a negatively curved DOPC structure might therefore result to some extent from greater flexibility as well as a change in spontaneous curvature.

Our results with DMPC should be interpreted with caution. At the conditions used here, GrA with DMPC induces greater disorder and a general acceleration of adsorption, but not formation of the H_{II} phase or any effect on adsorption from the interface. The similarities and differences between the two lipids therefore suggest that greater disorder in the lipid vesicles is sufficient to promote their adsorption, but that effects from the interface require structures with spontaneous curvature. The extent, however, to which GrA changes spontaneous curvature with DMPC remains unknown. DMPC with the peptide continues to form bilayers in which any curvature in the two individual leaflets would be cancelled by their opposite orientation. Although the results with DMPC generally agree with the model, they provide evidence that is less conclusive than suggested by superficial review.

Our results generally support adsorption via a negatively curved structure, but they do not exclude all other possibilities. A recently proposed model of fusion, for instance, suggests that two bilayers, brought into sufficiently close proximity by fusogenic proteins, might lack the intervening aqueous environment necessary to maintain the orientation of lipid constituents in the opposing leaflets [52]. The lipids might then simply flip. For a vesicle approaching an air–water interface, such a reorientation of constituents in the outer leaflet would produce the alignment required for a stable surface film. Although at least the initial vesicles would seem to lack a process that would drive approach to the interface close enough to cause the necessary dehydration, our results provide no evidence that contradicts this or other models. Our findings, however, do directly support models in which negative curvature is an important component of rate-limiting kinetic intermediates.

In summary, our results show that under conditions at which GrA stabilizes negatively curved structures with DOPC, the peptide also causes the same functional effects on the adsorption of DOPC that the hydrophobic surfactant proteins produce with the surfactant lipids. Our results support a model in which the hydrophobic proteins promote adsorption by stabilizing a rate-limiting structure with negative curvature that is intermediate between the vesicular bilayer and the interfacial film.

Acknowledgments

The authors thank Dr. Edmund Egan of ONY, Inc. for the gift of CLSE, Dr. David Peyton of Portland State University for the use of his NMR instrument, and N.A. Hannah for technical help in analysis of data from SAXS and NMR. These studies were funded by the National Institutes of Health (HL 54209).

References

1. Horie T, Hildebrandt J. Dynamic compliance, limit cycles, and static equilibria of excised cat lung. J Appl Physiol. 1971; 31:423–430. [PubMed: 5111861]
2. Schürch S, Goerke J, Clements JA. Direct determination of surface tension in the lung. Proc Natl Acad Sci U S A. 1976; 73:4698–4702. [PubMed: 1070020]
3. Valberg PA, Brain JD. Lung surface tension and air space dimensions from multiple pressure–volume curves. J Appl Physiol. 1977; 43:730–738. [PubMed: 578511]
4. Wilson TA. Relations among recoil pressure, surface area, and surface tension in the lung. J Appl Physiol. 1981; 50:921–930. [PubMed: 7228763]
5. Smith JC, Stamenovic D. Surface forces in lungs: I. Alveolar surface tension–lung volume relationships. J Appl Physiol. 1986; 60:1341–1350. [PubMed: 3754553]
6. Robertson, B. Pathology and pathophysiology of neonatal surfactant deficiency ("respiratory distress syndrome," "hyaline membrane disease". In: Robertson, B.; Van Golde, LMG.; Batenburg, JJ., editors. Pulmonary Surfactant. 1. Elsevier Science Publishers; Amsterdam: 1984. p. 383-418.
7. Lachmann B, Grossmann G, Nilsson R, Robertson B. Lung mechanics during spontaneous ventilation in premature and fullterm rabbit neonates. Respir Physiol. 1979; 38:283–302. [PubMed: 523846]
8. Nicholas TE, Power JH, Barr HA. The pulmonary consequences of a deep breath. Respir Physiol. 1982; 49:315–324. [PubMed: 7146654]
9. Wang Z, Hall SB, Notter RH. Roles of different hydrophobic constituents in the adsorption of pulmonary surfactant. J Lipid Res. 1996; 37:790–798. [PubMed: 8732779]
10. Nogee LM, Garnier G, Dietz HC, Singer L, Murphy AM, deMello DE, Colten HR. A mutation in the surfactant protein B gene responsible for fatal neonatal respiratory disease in multiple kindreds. J Clin Invest. 1994; 93:1860–1863. [PubMed: 8163685]
11. Clark JC, Wert SE, Bachurski CJ, Stahlman MT, Stripp BR, Weaver TE, Whitsett JA. Targeted disruption of the surfactant protein B gene disrupts surfactant homeostasis, causing respiratory failure in newborn mice. Proc Natl Acad Sci U S A. 1995; 92:7794–7798. [PubMed: 7644495]
12. Melton KR, Nesslein LL, Ikegami M, Tichelaar JW, Clark JC, Whitsett JA, Weaver TE. SP-B deficiency causes respiratory failure in adult mice. Am J Physiol, Lung Cell Mol Physiol. 2003; 285:L543–L549. [PubMed: 12639841]
13. Sen A, Hui SW, Mosgrober-Anthony M, Holm BA, Egan EA. Localization of lipid exchange sites between bulk lung surfactants and surface monolayer: freeze fracture study. J Colloid Interface Sci. 1988; 126:355–360.
14. Schürch S, Schürch D, Curstedt T, Robertson B. Surface activity of lipid extract surfactant in relation to film area compression and collapse. J Appl Physiol. 1994; 77:974–986. [PubMed: 8002555]
15. Haller T, Dietl P, Stockner H, Frick M, Mair N, Tinhofer I, Ritsch A, Enhorning G, Putz G. Tracing surfactant transformation from cellular release to insertion into an air–liquid interface. Am J Physiol, Lung Cell Mol Physiol. 2004; 286:L1009–L1015. [PubMed: 14704221]
16. Oosterlaken-Dijksterhuis MA, Haagsman HP, van Golde LMG, Demel RA. Interaction of lipid vesicles with monomolecular layers containing lung surfactant proteins SP-B or SP-C. Biochemistry. 1991; 30:8276–8281. [PubMed: 1868098]
17. Walters RW, Jenq RR, Hall SB. Distinct steps in the adsorption of pulmonary surfactant to an air–liquid interface. Biophys J. 2000; 78:257–266. [PubMed: 10620290]
18. Chernomordik L, Kozlov MM, Zimmerberg J. Lipids in biological membrane fusion. J Membr Biol. 1995; 146:1–14. [PubMed: 7563032]
19. Chernomordik L, Chanturiya A, Green J, Zimmerberg J. The hemifusion intermediate and its conversion to complete fusion: regulation by membrane composition. Biophys J. 1995; 69:922–929. [PubMed: 8519992]
20. Kozlov MM, Leikin SL, Chernomordik LV, Markin VS, Chizmadzhev YA. Stalk mechanism of vesicle fusion. Eur Biophys J. 1989; 17:121–129. [PubMed: 2792021]
21. Schram V, Hall SB. Thermodynamic effects of the hydrophobic surfactant proteins on the early adsorption of pulmonary surfactant. Biophys J. 2001; 81:1536–1546. [PubMed: 11509366]

22. Yu SH, Harding PGR, Possmayer F. Artificial pulmonary surfactant. Potential role for hexagonal H(II) phase in the formation of a surface-active monolayer. Biochim Biophys Acta. 1984; 776:37–47.
23. Perkins WR, Dause RB, Parente RA, Minchey SR, Neuman KC, Gruner SM, Taraschi TF, Janoff AS. Role of lipid polymorphism in pulmonary surfactant. Science. 1996; 273:330–332. [PubMed: 8662513]
24. Gruner SM. Stability of lyotropic phases with curved interfaces. J Phys Chem. 1989; 93:7562–7570.
25. Morrow MR, Stewart J, Taneva S, Dico A, Keough KMW. Perturbation of DPPC bilayers by high concentrations of pulmonary surfactant protein SP-B. Eur Biophys J Biophys Lett. 2004; 33:285–290.
26. Rajan S, Kang SY, Gutowsky HS, Oldfield E. Phosphorus nuclear magnetic resonance study of membrane structure. Interactions of lipids with protein, polypeptide, and cholesterol. J Biol Chem. 1981; 256:1160–1166. [PubMed: 6256387]
27. Killian JA. Gramicidin and gramicidin–lipid interactions. Biochim Biophys Acta. 1992; 1113:391–425. [PubMed: 1280467]
28. Bouchard M, Le Guerneve C, Auger M. Comparison between the dynamics of lipid/gramicidin A systems in the lamellar and hexagonal phases: a solid-state 13C NMR study. Biochim Biophys Acta. 1998; 1415:181–192. [PubMed: 9858726]
29. Kobayashi Y, Fukada K. Characterization of swollen lamellar phase of dimyristoylphosphatidylcholine-gramicidin A mixed membranes by DSC, SAXS, and densimetry. Biochim Biophys Acta. 1998; 1371:363–370. [PubMed: 9630724]
30. Notter RH, Finkelstein JN, Taubold RD. Comparative adsorption of natural lung surfactant, extracted phospholipids, and artificial phospholipid mixtures to the air–water interface. Chem Phys Lipids. 1983; 33:67–80. [PubMed: 6688762]
31. Hall SB, Wang Z, Notter RH. Separation of subfractions of the hydrophobic components of calf lung surfactant. J Lipid Res. 1994; 35:1386–1394. [PubMed: 7989863]
32. Ames BN. Assay of inorganic phosphate, total phosphate and phosphatases. Methods Enzymol. 1966; VIII:115–118.
33. King RJ, Clements JA. Surface active materials from dog lung: III. Thermal analysis. Am J Physiol. 1972; 223:727–733. [PubMed: 5068621]
34. Seelig J. ^{31}P nuclear magnetic resonance and the head group structure of phospholipids in membranes. Biochim Biophys Acta. 1978; 515:105–140. [PubMed: 356883]
35. Tournois H, Leunissen-Bijvelt J, Haest CW, de Gier J, de Kruijff B. Gramicidin-induced hexagonal HII phase formation in erythrocyte membranes. Biochemistry. 1987; 26:6613–6621. [PubMed: 2447938]
36. Killian JA, Burger KN, de Kruijff B. Phase separation and hexagonal HII phase formation by gramicidins A, B and C in dioleoylphosphatidylcholine model membranes. A study on the role of the tryptophan residues. Biochim Biophys Acta. 1987; 897:269–284. [PubMed: 2434129]
37. Tournois H, Fabrie CH, Burger KN, Mandersloot J, Hilgers P, van Dalen H, de Gier J, de Kruijff B. Gramicidin A induced fusion of large unilamellar dioleoylphosphatidylcholine vesicles and its relation to the induction of type II nonbilayer structures. Biochemistry. 1990; 29:8297–8307. [PubMed: 1701325]
38. Luzzati, V. X-ray diffraction studies of lipid–water systems. In: Chapman, D., editor. Biological Membranes. Academic Press; NY: 1968. p. 71-123.
39. Kohler SJ, Klein MP. Orientation and dynamics of phospholipid head groups in bilayers and membranes determined from ^{31}P nuclear magnetic resonance chemical shielding tensors. Biochemistry. 1977; 16:519–526. [PubMed: 556947]
40. Bocian DF, Chan SI. NMR studies of membrane structure and dynamics. Annu Rev Phys Chem. 1978; 29:307–335.
41. Schram V, Hall SB. SP-B and SP-C alter diffusion in bilayers of pulmonary surfactant. Biophys J. 2004; 86:3734–3743. [PubMed: 15189869]

42. Schram V, Anyan WR, Hall SB. Non-cooperative effects of lung surfactant proteins on early adsorption to an air/water interface. Biochim Biophys Acta. 2003; 1616:165–173. [PubMed: 14561474]
43. Oosterlaken-Dijksterhuis MA, Haagsman HP, van Golde LMG, Demel RA. Characterization of lipid insertion into monomolecular layers mediated by lung surfactant proteins SP-B and SP-C. Biochemistry. 1991; 30:10965–10971. [PubMed: 1932022]
44. Helfrich, W. Elasticity and thermal undulations of fluid films of amphiphiles. In: Charvolin, J.; Joanny, JF.; Zinn-Justin, J., editors. Liquides aux Interfaces=Liquids at Interfaces. North-Holland; Amsterdam: 1990. p. 209-237.
45. Helfrich W. Elastic properties of lipid bilayers: theory and possible experiments. Z Naturforsch, C. 1973; 28:693–703. [PubMed: 4273690]
46. Helfrich W. Size distribution of vesicles: the role of the effective rigidity of membranes. J Phys (Paris). 1986; 47:321–329.
47. Szule JA, Rand RP. The effects of gramicidin on the structure of phospholipid assemblies. Biophys J. 2003; 85:1702–1712. [PubMed: 12944285]
48. Rananavare SB, Ward AJI, Friberg SE, Larsen DW. Solvent–solute interactions in a liquid crystalline phase formed by ethylene glycol, water and lecithin. Mol Cryst Liq Cryst. 1986; 133:207.
49. Smith, ICP.; Ekiel, IH. Phosphorus-31 NMR of phospholipids in membranes. In: Gorenstein, DG., editor. Phosphorus-31 NMR: Principles and Applications. Academic Press; Orlando, FL: 1984. p. 447-475.
50. Sheng, P. Introduction to the elastic continuum theory of liquid crystals. In: Priestly, EB.; Wojtowicz, PJ.; Sheng, P., editors. Introduction to Liquid Crystals. Plenum Press; New York: 1975. p. 103-127.
51. Chandrasekhar, S. Liquid Crystals. Cambridge Univ. Press; New York, NY: 1992. p. 58
52. Tamm LK, Crane J, Kiessling V. Membrane fusion: a structural perspective on the interplay of lipids and proteins. Curr Opin Struct Biol. 2003; 13:453–466. [PubMed: 12948775]

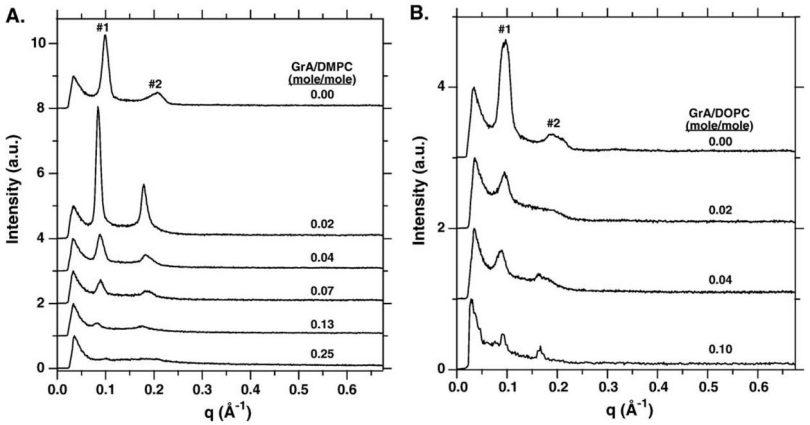

Fig. 1.

SAXS from dispersed samples of phospholipid with different amounts of GrA. Profiles were obtained with a constant phospholipid concentration of 30 mM in buffered saline (150 mM NaCl, 10 mM HEPES pH 7.0) at 37 °C. The first and second order diffraction peaks are labeled for phospholipid without GrA. For clarity of presentation, the curves for the different experiments are each shifted by a constant value of intensity. (A) DMPC. (B) DOPC.

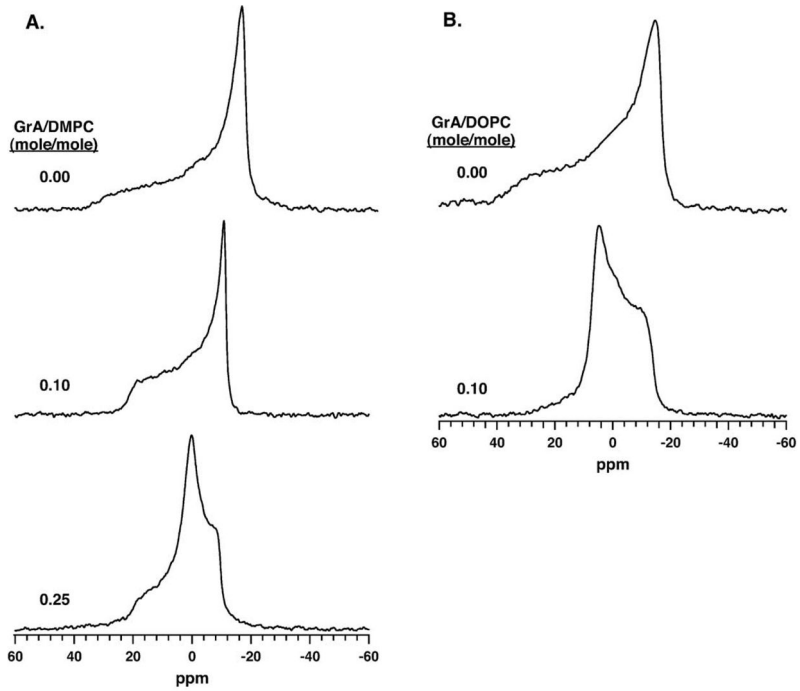

Fig. 2.

^{31}P-NMR spectra of phospholipid with and without GrA. Spectra were obtained with a constant phospholipid concentration of 30 mM in buffered saline (150 mM NaCl, 10 mM HEPES pH 7.0) at 37 °C. (A) DMPC. (B) DOPC.

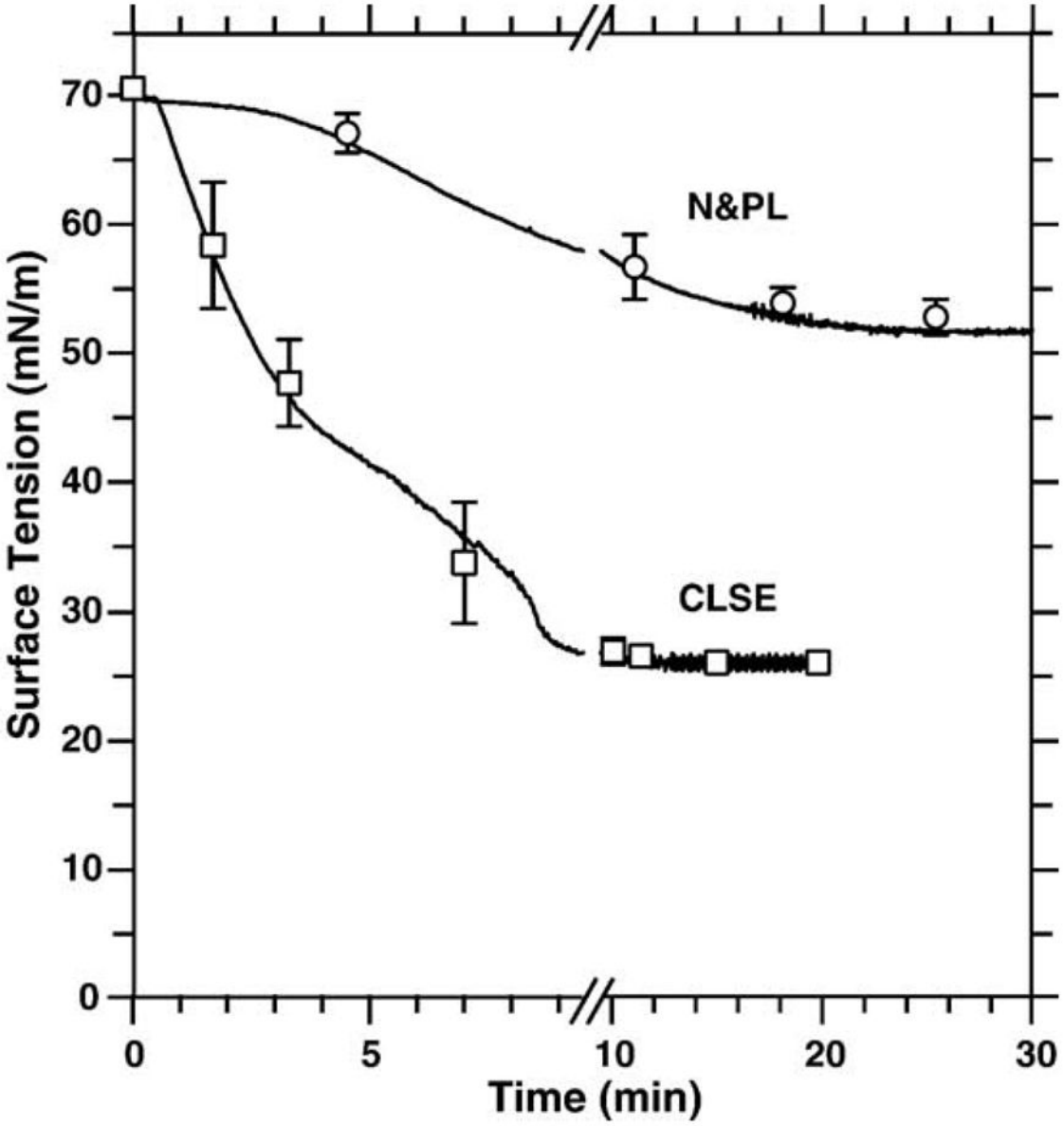

Fig. 3.

Adsorption of the pulmonary surfactant lipids in the presence (CLSE) and absence (N&PL) of the hydrophobic surfactant proteins. Curves show the variation of surface tension after removing the surface film from a dispersion of vesicles at 100 μM phospholipid and 37 °C in buffered saline with calcium (150 mM NaCl, 1.5 mM $CaCl_2$, 10 mM HEPES pH 7.0). Curves are representative of three experiments. Symbols give mean±S.D. at specific times to indicate the variance among different experiments.

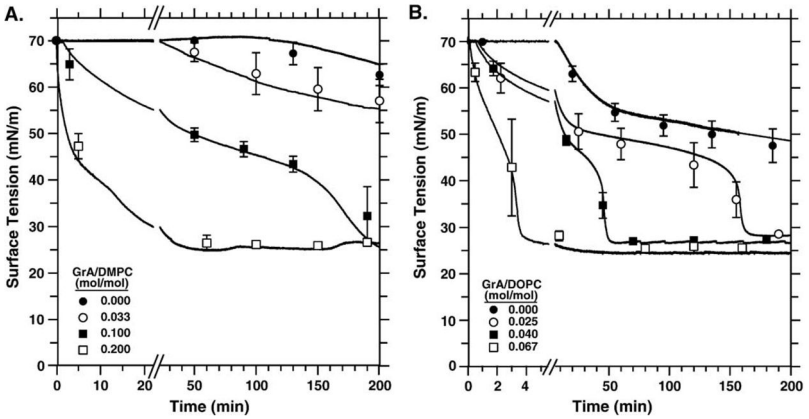

Fig. 4.

Adsorption to the air–water interface of phospholipid vesicles with different amounts of GrA. Experiments were performed at 150 μM phospholipid in buffered saline (150 mM NaCl, 10 mM HEPES pH 7.0) at 37 °C. Ratios of GrA/DOPC are mole/mole. Curves are representative of at least three experiments, with mean±S.D. shown at selected times. (A) DMPC. Data for GrA/DMPC of 0.02 and 0.07, which are omitted for clarity of presentation, fit in the sequence of curves according to the dose of GrA. (B) DOPC. Omitted data for GrA/DOPC of 0.02, 0.04, 0.10 similarly fit in the sequence of curves according to the dose of GrA.

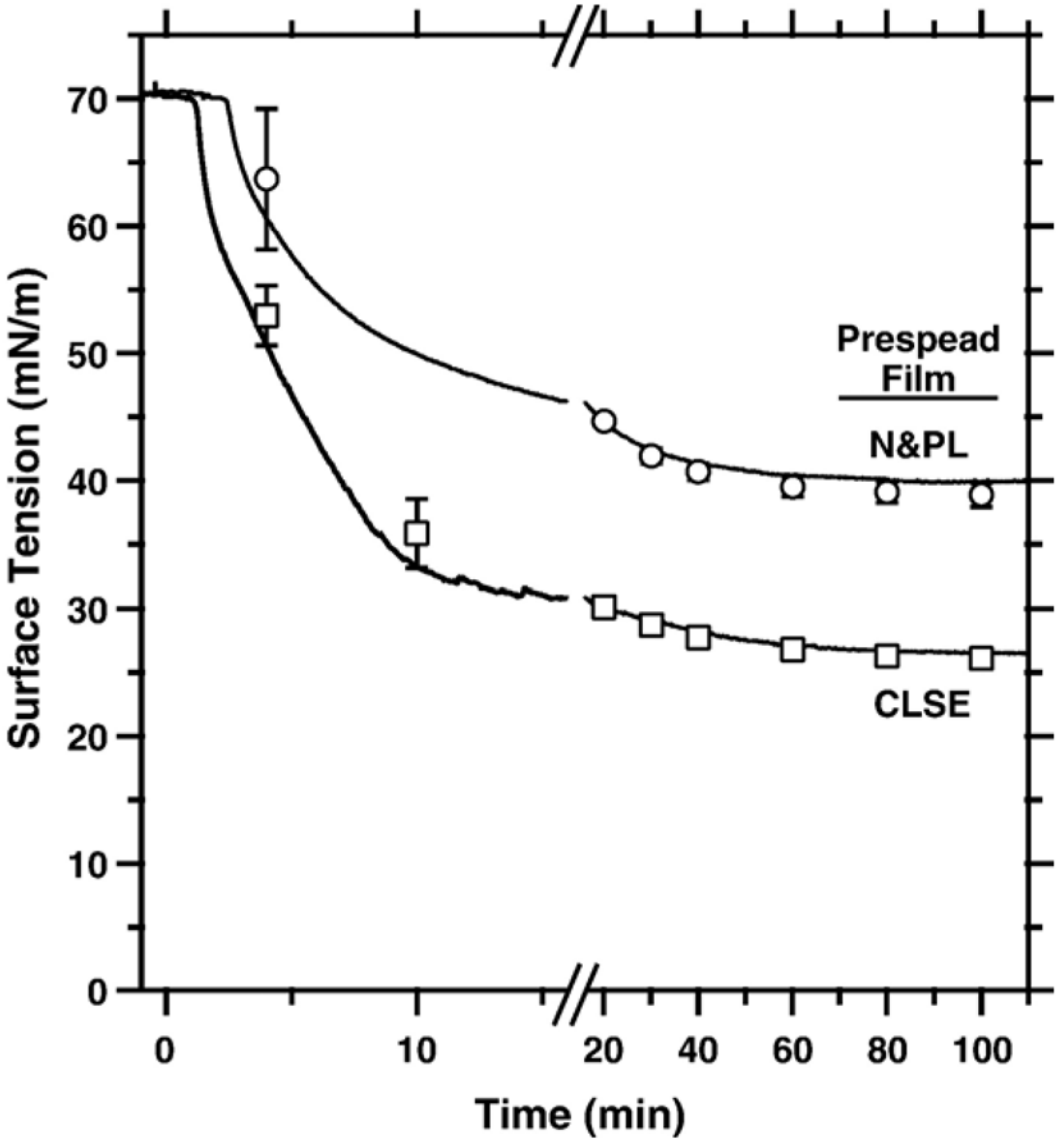

Fig. 5.

Adsorption of N&PL vesicles to prespread films with and without the hydrophobic surfactant proteins. Experiments were performed at 37 °C by injecting 100 μl vesicles of N&PL into a well-stirred subphase (150 mM NaCl, 1.5 mM $CaCl_2$, 10 mM HEPES pH 7.0) to a final concentration of 100 μM phospholipid below a preexisting film containing either N&PL or CLSE at 1.02 μmol/m^2 phospholipid. Curves are representative of at least three experiments. Symbols indicate the mean±S.D. at selected times.

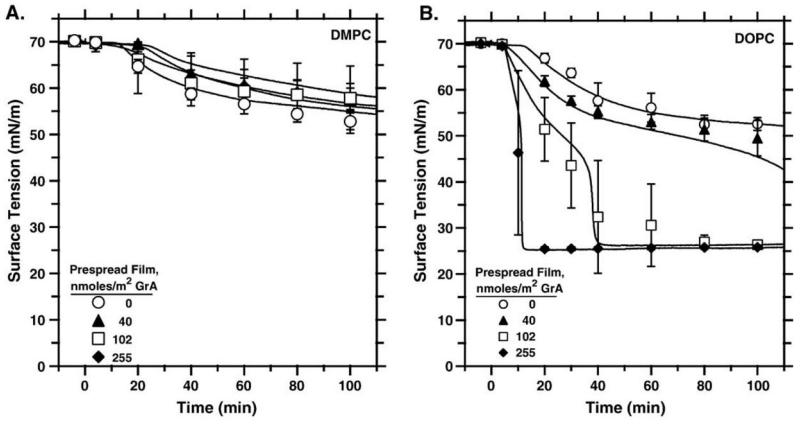

Fig. 6.

Adsorption of phospholipid vesicles to preformed phospholipid films containing different amounts of GrA. Experiments were performed at 37 °C by injecting 150 μl of lipid vesicles without GrA to a final concentration of 150 μM lipid into a well stirred subphase (150 mM NaCl, 10 mM HEPES pH 7.0) below a prespread film containing 1.02 μmol/m^2 phospholipid with different amounts of GrA. Curves are representative of at least three experiments. Symbols give the mean±S.D. at selected times. (A) DMPC. (B) DOPC.

Table 1

Quantitative data from SAXS for GRA–LIPID mixtures

(molar ratio)	q_1 nm^{-1}	q_2 nm^{-1}	d_1 nm	d_2 nm	d_1/d_2	I_1 (a.u.)
DMPC						
0	0.995±0.001	2.05±0.01	6.32±0.01	3.07±0.01	2.06±0.01	1.86±0.03
0.02	0.850±0.003	1.80±0.01	7.39±0.02	3.49±0.01	2.12±0.01	3.50±0.10
0.04	0.893±0.003	1.86±0.01	7.04±0.02	3.39±0.01	2.08±0.01	0.78±0.02
0.07	0.896±0.003	1.87±0.01	7.01±0.03	3.36±0.02	2.09±0.02	0.38±0.02
0.13	0.818±0.006	1.77±0.01	7.68±0.06	3.55±0.02	2.16±0.03	0.13±0.02
DOPC						
0.00	0.958±0.003	1.94±0.01	6.56±0.02	3.24±0.02	2.03±0.02	1.38±0.03
0.02	0.949±0.003	1.85±0.01	6.62±0.03	3.40±0.20	2.00±0.10	0.34±0.02
0.04	0.878±0.003	1.65±0.02	7.16±0.03	3.80±0.03	1.88±0.02	0.30±0.02
0.07	0.905±0.003	1.65±0.01	6.94±0.03	3.80±0.01	1.83±0.01	0.39±0.02
0.10	0.920±0.010	1.66±0.01	6.82±0.03	3.78±0.03	1.80±0.03	0.21±0.06

The numbered subscripts indicate values for the first and second order diffractions peaks for *q*-spacing, *d*-spacing and intensity (*I*). Values are the best fit to a Gaussian function±3 S.D. with respect to the fitting function.

Table 2

NMR analysis of DOPC mixed with GRA

GrA/lipid (mol/mol)	Chemical shift anisotropy (ppm)		Lamellar volume fraction
	Lamellar	**Isotropic**	
DMPC			
0.00	−46.4±0.2	–	–
0.10	−33.5±0.2	–	–
0.25	−27.5±0.1	−0.05±0.03	0.78±0.03
GrA/lipid (mol/mol)	Chemical shift anisotropy (ppm)		Lamellar volume fraction
	Lamellar	Hexagonal	
DOPC			
0.00	−46.7±0.2	–	1.00
0.10	−41.3±0.2	18.3±0.1	0.21±0.01

Data are best-fit values±3 S.D. with respect to the fitting function.